To appear in Bioinspiration and Biomimetics

The significance of moment-of-inertia variation in flight manoeuvres of butterflies

T. Lin[1], R. Mittal[1], L. Zheng[1], T. Hedrick[2]

[1]Department of Mechanical Engineering, The Johns Hopkins University, 3400 N Charles Street, Baltimore, MD 21218, USA

[2]Department of Biology, University of North Carolina at Chapel Hill, CB 3280, Chapel Hill, NC 27599, USA

E-mail: mittal@jhu.edu

Abstract. The objective of this study is to understand the role that changes in body moment-of-inertia might play during flight manoeuvres of insects. High-speed, high-resolution videogrammetry is used to quantify the trajectory and body conformation of Painted Lady butterflies during flight manoeuvres; the 3D kinematics of the centre-of-masses of the various body parts of the insect are determined experimentally. Measurements of the mass properties of the insect are used to parameterize a simple flight dynamics model of the butterfly. Even though the mass of the flapping wings is small compared to the total mass of the insect, these experiments and subsequent analysis indicate that changes in moment-of-inertia during flight are large enough to influence the manoeuvres of these insects.

1. Introduction

Micro-aerial vehicles (MAV) are being designed for a variety of missions including environmental monitoring, reconnaissance, and search-and-rescue. In developing these MAVs, there is much that can be learned from insects because evolution has created an incredible variety of flying insects that have successfully colonized almost all known terrestrial habitats. One area where MAV design could learn from insects is in stabilization and manoeuvrability. The established method for studying these features in insects is to develop dynamic models that incorporate relevant details regarding mass properties, wing kinematics, and aerodynamic forces; these models are then used to explore the stability [4, 9, 11] and manoeuvrability of insects.

In all of the above studies however, the moment-of-inertia (MoI) of an insect is assumed to be constant in time. Insect bodies consist of the head, thorax, abdomen, and wings, and the assumption of time-invariant MoI for a flying insect is based on two underlying assumptions: the general assumption that the wings – which typically constitute a very small fraction of total body mass – do not contribute much to the MoI and the assumption that the head and body (thorax and abdomen) is a rigid entity that cannot change its shape. With regard to the former, while it is certainly true that wings typically account for a very small fraction of the total body mass, they might account for a larger fraction of the MoI since the moment arm of the wings about the centre-of-mass (CoM) can be large. Indeed, the roll and yaw MoI of larger flying animals such as birds and bats are dominated by wing inertia, which accounts for more than 90% of the total MoI of these animals [12, 13]. This, coupled with the flapping motion of the wings, could lead to non-negligible variations in MoI during flight. With regard to the latter, insects such as butterflies and moths show noticeable articulation of their abdomen and thorax during flight [2], and this could also result in a time-varying MoI.

The implications of time variation in MoI for insect flight are potentially significant. The balance of angular momentum states that,

$$[I]\,\ddot{\boldsymbol{\theta}} + [\dot{I}]\dot{\boldsymbol{\theta}} = \boldsymbol{\tau} \tag{1}$$

where $\boldsymbol{\tau}$ is torque, $[I]$ is the moment-of-inertia tensor, and $\dot{\boldsymbol{\theta}}$ is the angular velocity. If the MoI is assumed to be time-invariant, then the second term on the left-hand-side of the above equation vanishes. If however, the rate-of-change of the MoI is significant enough such that the second term is non-negligible, then the dynamics of flight can potentially be affected. In particular, the insect could modulate its angular velocity by changing its MoI, and thereby enhance its manoeuvrability. In addition, a time-varying MoI may change the flight stability characteristics of the insect.

The objective of the current study is to assess the importance of MoI variation in insect flight manoeuvres. In particular, we attempt to evaluate the magnitude of the terms on the left-hand-side of equation (1) for a butterfly in free-flight and draw conclusions regarding the potential importance of moment-of-inertia variation during a typical flight manoeuvre.

2. Methods and Procedures

The insect species chosen for the current research is the Painted Lady (*Vanessa cardui*) shown in figure 1(a). Butterflies have excellent manoeuvrability and flight characteristics, and while these insects have large wings, they constitute less than 10% of the total body mass. The Painted Lady species has been chosen because they are simple to obtain and maintain, and they remain in reasonable condition for flight experiments for about two weeks when kept in the laboratory. Wing flapping frequencies are about 20 - 25 Hz and the average wing-span of the specimens chosen for our study is about 7 cm. In forward flight and climbing flight, the Reynolds numbers are 3,455 and 3,528, respectively (based on the wing length and mean wingtip velocity), and the Strouhal numbers are 0.37 and 0.60, respectively (based on the mean chord length and mean heading velocity).

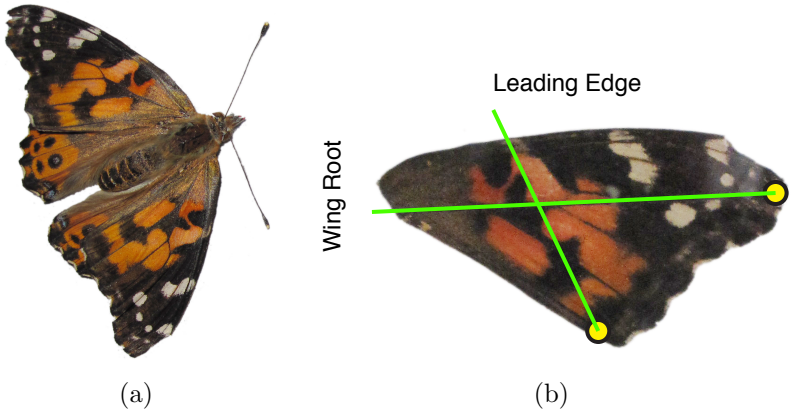

Figure 1. (a) Painted Lady butterfly (b) Centre-of-mass of a forewing determined using two plumb-lines (circles indicate the two hinge points).

Estimation of the centre-of-mass and the moment-of-inertia of the insect requires an estimation of the centre-of-mass of each component of the insect body. The CoMs of the head and body (body comprises of the abdomen and thorax) are found by locating the volume-centroid of each segment using Adobe Photoshop. The underlying assumption here is that the body density does not vary within each segment. The wings however, cannot be assumed to have a uniform density due to the concentration of large veins near the wing root and the leading edge of the wing. However, each wing can be assumed to be a lamina for which the CoM can be found by using the plumb-line method [8]. Each wing is pinned to a board with a needle (where it can rotate freely), and a plumb-bob is hung from the needle with a piece of string. The intersection of the string with the wing is recorded with a camera. The wing is then rotated and pinned to the board in a different orientation. The same procedure is repeated, and the two images are superimposed on top of each other in Adobe Photoshop; the intersection of the two strings is the CoM. Figure 1(b) shows the identification of the CoM for a forewing, and it is clear that the CoM is closer to the wing root and leading edge than the centroid is.

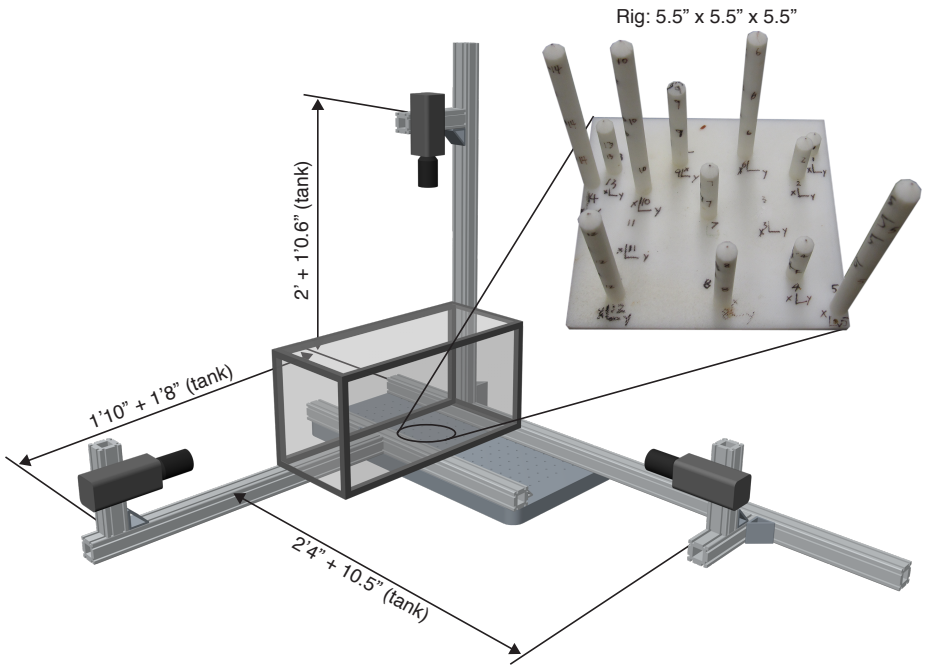

Figure 2. Videogrammetry setup with approximate dimensions showing three high-speed cameras and the flight chamber. Also shown is the calibration rig used for the DLT analysis.

The insect flight videogrammetry setup is shown in figure 2. The Painted Lady butterflies are kept in a separate glass enclosure and then transferred to the main glass chamber prior to experiments. The butterflies fly inside the main glass chamber and three synchronized Redlake Y4L high-speed cameras paired with Nikon AF Nikkor 24-85mm f/2.8 - 4D IF close-focusing lenses are used to capture videos of the butterflies in free-flight. Because the flapping frequency of the Painted Lady butterfly is around 20 - 25 Hz, recording frame rates ranging from 2,000 - 3,000 frames per second and a shutter speed of 150 μs are used to capture a sharp image of the butterfly at each frame. In order to maintain an appropriate depth-of-field in each of the videos, a lens f-stop of at least f/11 is used. Due to these exposure constraints, the chamber is illuminated intensely with multiple halogen lights to maintain the required exposure of the video cameras. The three cameras are calibrated in three dimensions with a prototyped calibration rig (shown in figure 2) that is photographed at the end of each recording session. The rig was prototyped with a precision of 0.25 mm to ensure that the spatial coordinates of the CoMs of the various body parts of the butterfly during a manoeuvre could be extracted with sufficient accuracy. The cameras were calibrated using direct linear transformation (DLT) [1], which uses the known 3D locations of the control points in the calibration rig and their pixel positions in the image to solve for a set of coefficients which describe the camera pose, position, and lens properties in the rig coordinate system. Coefficients and pixel coordinates from two or more cameras may then be used to reconstruct a 3D

location using a set of linear equations. The calibration root-mean-square error was 0.22 pixels in this case, which is approximately 0.07 mm. This setup provides us with acceptable temporal and spatial resolution of the butterfly in flight.

Various flight manoeuvres are induced using sugar water and fresh foliage. The recorded sequences of video are then saved onto a desktop computer for analysis. Segments of videos that contain distinct and clearly visible flight behaviour are selected for detailed analysis. Using the DLT toolkit developed by Hedrick (2008) [6], the trajectories of the CoMs of the various body parts of the butterfly can be determined with accuracy in time and space. The naturally occurring patterns and features on the butterfly wings and body are identified in video frame pairs and DLT is used to extract the 3D spatial coordinates of these points on the butterfly.

3. Results and Discussion

Our mass model of the butterfly is comprised of six parts: two front wings, two hind wings, the head, and the body (abdomen and thorax). Knowing the mass and spatial properties of the butterfly during a free-flight manoeuvre, the MoI about the CoM of the insect with respect to a fixed frame-of-reference (frame XYZ) can be computed at any time-instance during flight. The measured masses and standard deviations (S.D.) of the various body parts of a batch of six Painted Lady butterflies are shown in table 1. It is noted the total mass of the four wings constitutes only about 7% of the total mass of the butterfly; this underpins the generally accepted notion that the wings do not contribute much to the rotational MoI of the insect [3].

Table 1. Masses and standard deviations of the body parts of a set of six Painted Lady butterflies.

Body Part	Average Mass ± S.D. [mg]
Single forewing	3.86 ± 0.28
Single hindwing	3.19 ± 0.23
Head	9.0 ± 1.6
Body (abdomen & thorax)	177.1 ± 32.6
Total	200.2 ± 35.22

Our analysis of moment-of-inertia variation during flight is based primarily on forward flight recordings. This flight mode is relatively common and easy to capture in a laboratory setting. Furthermore, as opposed to manoeuvres, the wing beats during forward flight are expected to be relatively periodic and repeatable, making them more amenable to statistical analysis. Due to the bilateral anatomical symmetry of the butterfly about its sagittal plane, the principal axes obtained from a spectral decomposition of the MoI tensor constitute the roll, pitch, and yaw axes, and the eigenvalues are the corresponding moments-of-inertia. In the current study, we have selected one particular segment from a recorded video of about four wing flaps of the

Painted Lady butterfly in forward flight for detailed analysis; the principal moments-of-inertia calculated from this segment are shown in figure 3. Using the measurement uncertainty of the DLT analysis [6] for each of the body segment CoMs, the standard deviation of the location of the CoM of the entire insect was determined to be 0.19 mm in the X direction, 0.23 mm in the Y direction, and 0.15 mm in the Z (elevation) direction. In addition, as shown in figure 3, the standard deviations of the moments-of-inertia are calculated at three different times: at the beginning of a downstroke (a), mid-downstroke (b), and at the end of the downstroke (c). These standard deviations were approximately 3% of the magnitude of the moments-of-inertia.

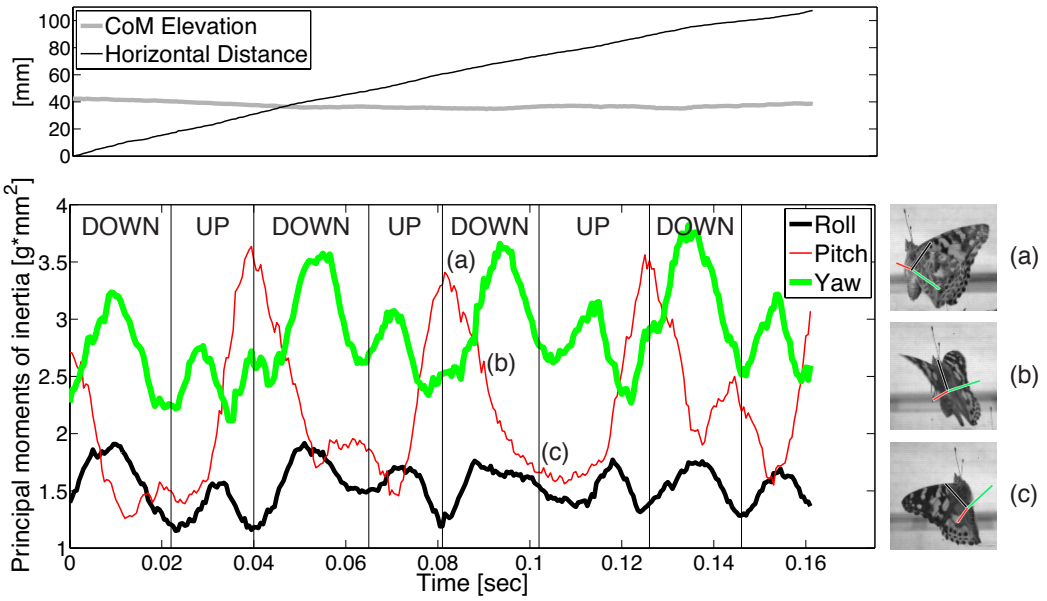

	Mean [g·mm^2]	Variation (% of mean)	S.D. (a) [g·mm^2]	S.D. (b) [g·mm^2]	S.D. (c) [g·mm^2]
Roll MoI	1.54	0.62 (40.3%)	0.04	0.06	0.04
Pitch MoI	2.19	2.07 (94.5%)	0.09	0.06	0.07
Yaw MoI	2.85	1.40 (49.1%)	0.10	0.08	0.08

Figure 3. Temporal variation of the principal moments-of-inertia for a Painted Lady butterfly in forward flight over four wing flaps. Also shown are the time-mean values over the four wing flaps and the average variations that occur over each wing flap for each of the principal moments-of-inertia. The standard deviations are calculated for each of the principal moments-of-inertia at times (a), (b), and (c); time (a) corresponds to 0.0815 sec, time (b) corresponds to 0.0935 sec, and time (c) corresponds to 0.101 sec. In addition, the elevation of the insect CoM and the horizontal distance travelled by the CoM are plotted above.

The plot in figure 3, as well as the tabulated data, lends itself to a number of interesting observations. Based on the time-mean values of the MoI, the yaw MoI is the highest among the three principal moments, whereas the roll MoI is the lowest. The low value of the roll MoI is owing to the fact that the head, thorax, and abdomen, which constitute most of the mass of the insect, do not contribute as much to this

component of the MoI. It is also clear from the plots that there is substantial temporal variation in the moment-of-inertia of the butterfly along all three principal directions. In particular, the largest variation in MoI is observed along the pitch-axis with values oscillating between about 1.46 and 3.53 g·mm^2 in approximately 0.02 seconds, or half a flapping cycle. It should be noted that this overall variation of 2.07 g·mm^2 is very close to the mean value of 2.19 g·mm^2 for this MoI component. For the yaw and roll MoI, the range of variation is about 49.1% and 40.3%, respectively, of the corresponding mean values. Most of these large variations in the MoI come from the motion of the wings and clearly indicate that despite the relatively small mass of the wings, the wings actually contribute substantially to all three principal moments-of-inertia. The mean moments-of-inertia calculated for the butterfly are consistent with those expected for a flying animal of its size [7], suggesting that these findings may be broadly characteristic of other large and medium size insects.

It is also apparent that the yaw MoI reaches a local maximum approximately when the butterfly's wings are stretched horizontally, and that the maxima are greater during the downstroke than during the upstroke. The pitch MoI reaches a local maximum at the end of each downstroke and upstroke; however, the pitch MoI attained at the end of an upstroke is greater. The yaw and roll MoI attain maxima and minima at approximately the same time, while the maxima and minima of the pitch MoI are shifted in phase by approximately half of a wingbeat.

It is also worth noting that while many of the features in the MoI temporal variation are similar from cycle-to-cycle, there are also some noticeable cycle-to-cycle variations. While some of this can be attributed to measurement uncertainties and errors, our observations indicate that some of these variations are due to actual changes in the wing kinematics and body conformations. Thus, even though the insect is seemingly flying in the forward direction during this segment, there are still some cycle-to-cycle variations in wing and body kinematics.

We have so far established that despite the relatively small ($\sim$7%) contribution of the wings to the overall mass, the wings contribute significantly to the moment-of-inertia of the insect. We have also shown that wing flapping results in a significant temporal variation of the MoI. We now extend this analysis to assess the potential impact of this changing moment-of-inertia on the manoeuvring of these insects.

Figure 4 shows the trajectories of the CoMs of the fore and hindwings calculated using DLT analysis, along with the roll, pitch, and yaw axes fixed to the CoM of a butterfly that is transitioning from forward to climbing flight. The trajectories of the CoMs of the wings confirm that the manoeuvre is indeed largely bilaterally symmetric. The two frames in figure 4 also show the principal axes at two instances of a flapping cycle.

Our assessment of the significance of the MoI variation during this flight manoeuvre are based on the equation,

$$I_p\ddot{\theta}_p + \dot{I}_p\dot{\theta}_p = \tau_p \tag{2}$$

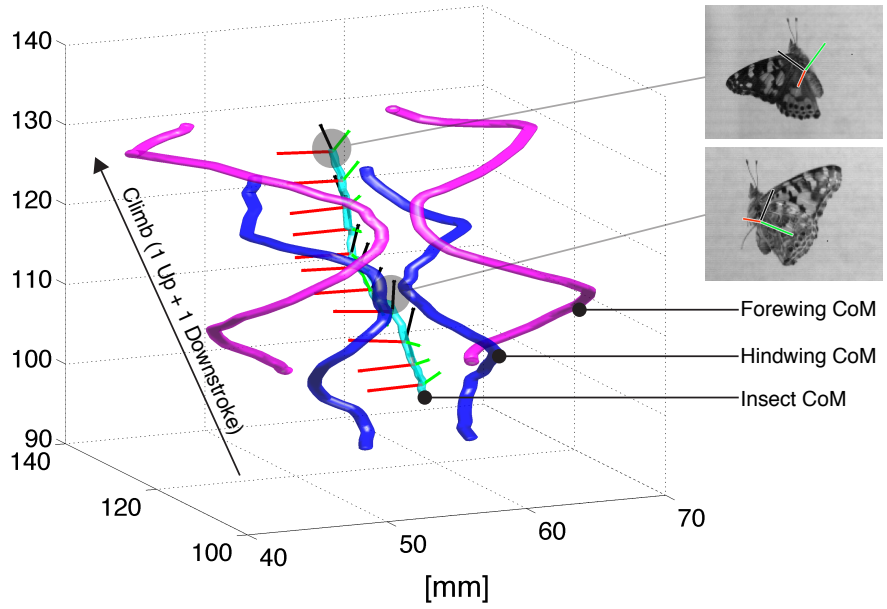

Figure 4. Spatial and temporal variation of the CoMs of the forewings, hindwings, and the insect over one upstroke and one downstroke during climbing flight. Also shown are the principal axes of the MoI tensor fixed to the CoM of the insect; the time duration between each set of principal axes shown is 0.005 sec.

where $\dot{\theta}_p$ and $\ddot{\theta}_p$ are the pitch-rate and pitch-acceleration, respectively, I_p is the pitch MoI, and τ_p is the pitching moment. Our objective is to estimate the relative magnitude of the two terms on the left-hand-side of equation (2). The pitch-angle θ_p of the butterfly during this manoeuvre is estimated as follows: the axis running through the head of the insect and the CoM of its body (defined here as the body-axis) is extracted using the DLT algorithm, and the angle created by the body-axis at each time-instance during the manoeuvre and the body-axis at the first video frame at the start of the manoeuvre is determined. It is important to note that the body-axis defined here is not necessarily coincident with what we identify here as the roll axis. From the beginning of a downstroke to the beginning of an upstroke, the principal roll axis creates an angle ranging from approximately $+40°$ to $-20°$ with the body-axis; this angle is approximately $0°$ near mid-downstroke and mid-upstroke.

Figure 5 shows the body pitch-angle estimated from this experimental procedure. The time variation of the body pitch-angle clearly shows a change of about 0.75 rad ($43°$) in body pitch-angle, corresponding to a transition from forward to climbing flight. The pitch-angle also exhibits cycle-to-cycle variations (which are associated with the wing flapping) as well as other small amplitude but high-frequency variations (which are likely due to experimental uncertainties). All of these variations can significantly contaminate the estimates of angular velocity and acceleration. In order to mitigate these effects and extract the large-scale features of the angular motion during this manoeuvre, we low-pass filter the above data by determining the mean angular position of the body-

axis during each wing flapping cycle and fit a smooth 4th-degree polynomial through these points as shown in figure 5. The pitch-rate $\dot{\theta}_p$ and pitch-acceleration $\ddot{\theta}_p$ are then calculated by computing the first and second derivatives of this smoothed pitch-angle using a one-sided finite-difference scheme as shown in figure 5.

From this figure, it is clear that the butterfly's maximum rate of pitch is about 8 rad/sec while its angular acceleration reaches magnitudes up to 300 rad/sec^2. This large disparity between the two quantities has provided an additional justification for neglecting the second term on the left-hand-side of equation (2) in the analysis of insect flight dynamics. However, this presupposes that the rate-of-change of MoI is of the same order of magnitude as the MoI itself, and we explore this issue using the current data.

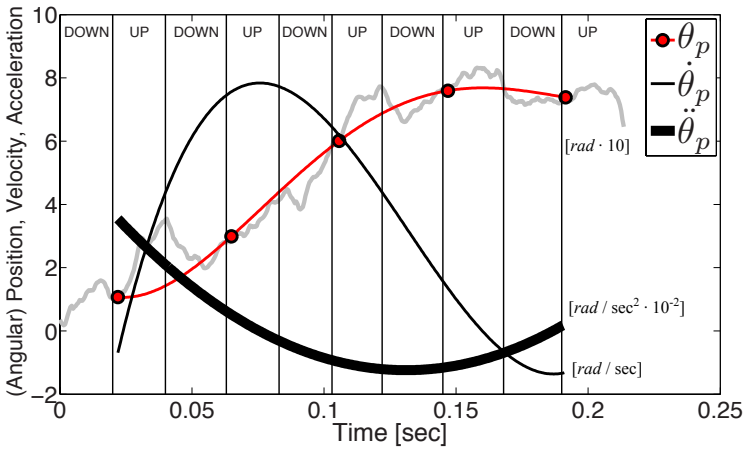

Figure 5. Pitch-angle θ_p, rate $\dot{\theta}_p$, and acceleration $\ddot{\theta}_p$ estimated for a butterfly undergoing a manoeuvre that transitions from forward to climbing flight. Note that the pitch-angle is scaled by a factor of 10 and the pitch-acceleration is scaled by a factor of 10^{-2}.

In order to conduct this analysis, we estimate I_p and $\dot{I}_p$ from the data corresponding to forward flight. Since the overall changes in MoI are mostly due to the flapping wings, we expect that these variations are approximately similar to those observed during a bilaterally symmetric manoeuvre such as the transition from forward flight to climbing flight that is described above. The MoI estimates for the forward flight case are more robust given that they are accumulated over four similar, consecutive flapping cycles. The bilateral symmetry of both the forward flight and the climbing manoeuvre, coupled with the fact that the MoI variation is produced primarily by the flapping of the wings – which is quite similar for both cases – provides justification for this approach.

For I_p, we estimate two values of 1.46 and 3.53 g·mm^2 that represent averages of the minima and maxima, respectively, of this parameter from the data in figure 3. For $\dot{I}_p$, we estimate a value of 2.07 g·mm^2 / 0.02 s = 103.5 g·mm^2/s which represents the average rate-of-change of pitch MoI during each half-stroke of the flapping cycle. We note that $\dot{I}_p$ is two orders of magnitude larger than I_p, indicating that the second term in equation (2) might not be negligible.

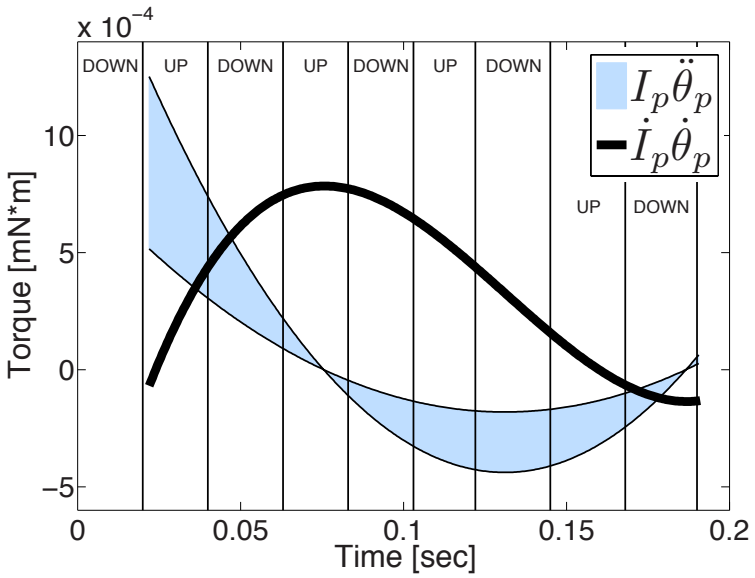

Figure 6. Components of rate-of-change of pitch angular momentum estimated using the upper and lower-bound of pitch MoI and the maximum time rate-of-change of MoI. Note that since the sign of $\dot{I}_p$ changes within each flapping cycle, the effect of $\dot{I}_p\dot{\theta}_p$ may be positive or negative throughout the manoeuvre.

In order to fully explore the relative magnitudes of the two terms on the left-hand-side of equation (2), we estimate the time variation of the two terms for the climbing manoeuvre with the chosen (fixed) values of I_p and $\dot{I}_p$ and the time varying values of pitch-rate and acceleration taken from the polynomial fits shown in figure 5. The resulting variation of these two terms is shown in figure 6 with the variation of the first term shown as a band of possible values corresponding to the two extrema of I_p. This plot shows that during this manoeuvre, the magnitudes of the torque component due to angular acceleration and the torque component due to the time rate-of-change of moment-of-inertia are quite comparable. Thus, even though the wings of the Painted Lady butterfly only contribute to about 7% of the total mass of the insect, the MoI changes induced by the movement of the wings likely affects the instantaneous dynamics of the insect during flight manoeuvres. This effect therefore cannot be neglected without proper justification in insect flight dynamics studies. It remains to be studied if (and how) insects make use of this additional torque component during the many rapid, and oftentimes complex, manoeuvres that they exhibit in natural flight. Because insects lack within-wing joints, wholly inertial reorientations such as those implicated in vertebrate flight [5] are likely of less importance, but interactions between external aerodynamic torques and inertial torques within the wingbeat cycle may substantially influence insect flight manoeuvres. For example, an aerodynamic roll torque applied at mid-downstroke might result in little immediate roll acceleration due to the high roll MoI of the butterfly at that time, but roll acceleration would continue through the remainder of the downstroke due to the rapid decline in roll MoI, leading to a large net change in

orientation. It would also be of interest to extend this understanding to the design of flapping wing micro-aerial vehicles in the future.

Acknowledgments

RM would like to acknowledge support from NSF and AFOSR for this research.

References

[1] Abdel-Aziz, Y.I., Karara, H.M., Direct linear transformation into object space coordinates in close-range photogrammetry. *Proc. Symp. on Close-Range Photogrammetry*, University of Illinois at Urbana-Champaign (1971).

[2] Chakravarthy, A., Albertani, R., Gans, N., Evers, J., Experimental Kinematics and Dynamics of Butterflies in Natural Flight, *Proceedings of 47th AIAA Aerospace Sciences Meetings*, January 5-8, 2009, Orlando, FL, Paper No. AIAA 2009-873.

[3] Dudley, R. Mechanisms and Implications of Animal Flight Maneuverability. *Integ. Comp. Biol.*, 42: 135-140 (2002).

[4] Gao, N., Aono, H., Liu, H., A Numerical Analysis of Dynamic Flight Stability of Hawkmoth Hovering. *Journal of Biomechanical Science and Engineering* 4: 105-116 (2009).

[5] Hedrick, T.L., Usherwood, J.R., Biewener, A.A., Low speed maneuvering flight of the rose-breasted cockatoo (Eolophus roseicapillus). II. Inertial and aerodynamic reorientation. *Journal of Experimental Biology* 210: 1897-1911 (2007).

[6] Hedrick, T.L., Software techniques for two- and three-dimensional kinematic measurements of biological and biomimetic systems. *Bioinspiration & Biomimetics* 3, 034001 (2008).

[7] Hedrick, T.L., Damping in flapping flight and its implications for manoeuvring, scaling and evolution. *Journal of Experimental Biology* 214: 4073-4083 (2011).

[8] Kleppner, D., Kolenkow, R., *An Introduction to Mechanics* (2nd ed.), McGraw-Hill, ISBN 0-07-035048-5 (1973).

[9] Sun, M., Wang, J.K., Flight Stabilization Control of a Hovering Model Insect. *Journal of Experimental Biology* 210: 2714-2722 (2007).

[10] Sun, M., Xiong, Y., Stabilization Control of a Bumblebee in Hovering and Forward Flight. *Acta Mech Sin* 25: 13-21 (2009).

[11] Taylor, G.K., Thomas, A.L.R., Dynamic flight stability in the desert locust Schistocerca gregaria. *Journal of Experimental Biology* 206: 2803-2829 (2003).

[12] Thollesson, M., Norberg, U.M., Moments of Inertia of Bat Wings and Body. *Journal of Experimental Biology* 151: 19:35 (1991).

[13] Van den Berg, C., Rayner, J.V.M., The moment of inertia of bird wings and the inertial power requirement for flapping flight. *Journal of Experimental Biology* 198: 1655-1664 (1995).